JOURNAL OF CATALYSIS 14, 142–147 (1969)

Diffusion Kinetics within Supported Liquid-Phase Catalysts

PETER R. RONY

From the Central Research Department, Monsanto Company, St. Louis, Missouri 63166

Received October 15, 1968; revised January 13, 1969

The homogeneous hydroformylation of propylene by butyl benzyl phthalate solutions of $(Ph_3P)_2Rh(CO)Cl$ was successfully used as a model reaction system to demonstrate the existence of an optimum liquid loading in supported liquid-phase catalysts (SLPC). The experimental results were consistent with a theoretical treatment of supported liquid-phase catalyst systems.

Introduction

Recently, Acres, Bond, Cooper, and Dawson (*1*) and the author (*2*) have independently demonstrated the feasibility of dispersing nonvolatile liquid catalyst solutions containing metal complexes within porous solids and performing vapor-phase reactions over fixed beds of such catalysts. This technique has general applicability and differs quite markedly from conventional catalyst dispersion techniques, such as mechanical agitation or gas sparging. For example, when employed in fixed- or fluidized-bed reactors, supported liquid-phase catalysts (SLPC), as the above hybrid catalysts are called, eliminate severe reactor corrosion problems; reduce the difficulties with the separation of, loss of, and fouling by valuable homogeneous catalysts; create higher gas–liquid interfacial areas and smaller liquid-phase diffusion paths; and reduce the difficulties of product separation. Such catalysts are particularly convenient for the laboratory screening of catalyst solutions.

Despite the fact that the SLPC dates as far back as 1935 (*3*, *4*), little is known about the physical characteristics of such catalyst composites. We have recently published a theory describing the steady state diffusion kinetics within such catalysts that predicts the existence of an optimum loading of the liquid catalyst solution corresponding to the point at which the SLPC has its greatest overall catalytic efficiency (*5*). In this paper, we will describe experiments which verify this prediction.

The reaction chosen for these studies was the homogeneously catalyzed hydroformylation of propylene

$$C_3H_8 + CO + H_2 \xrightarrow{(Ph_3P)_2Rh(CO)Cl} CH_3—CH_2—CH_2—CHO + CH_3—\underset{\displaystyle CH_3}{CH}—CHO$$

The catalyst for this reaction, bis(triphenylphosphine)rhodium carbonyl chloride, $(Ph_3P)_2Rh(CO)Cl$, was first reported by Osborn, Wilkinson, and Young (*6*). This reaction system had several advantages over other recently discovered homogeneous catalyst systems (*7–9*): the catalyst was more stable, the reaction was fast, and all of the reactants and products were gases at reaction conditions (*10*).

Nomenclature

a	Coefficient in Eq. (7)
D_{gas}	Gas-phase diffusion coefficient (cm^2/sec)
D_{liq}	Liquid-phase diffusion coefficient (cm^2/sec)
E_{ov}	Overall effectiveness factor
E_1	Effectiveness factor for a supported liquid-phase catalyst
F	Gas-phase flow rate in reactor void volume (cm^3 gas/sec)

k'	Liquid-phase pseudo-first-order rate constant (sec^{-1})
l	Average pore length (cm)
n	Exponent in Eq. (7)
p_i	Partial pressure of reactant at reactor inlet (atm)
p_o	Partial pressure of reactant at reactor outlet (atm)
V_{liq}	Total liquid volume in reactor (cm^3)
δ_{liq}	Experimental liquid loading (cm^3 liquid/cm^3 pore volume)
ϵ_{gas}	Volume ratio (cm^3 gas in region I/cm^3 pore volume in region I)
$\epsilon_{liq} = 1 - \epsilon_{gas}$	Volume ratio (cm^3 liquid in region I/cm^3 pore volume)
η	Dimensionless axial coordinate (Fig. 1)
$1/\eta_f$	Gas film diffusion resistance (*11*)
θ	Volume ratio (cm^3 liquid in region II/cm^3 pore volume) (Fig. 1)
κ_1	Gas–liquid partition coefficient (moles/cm^3 liquid: moles/cm^3 gas)
μ	Dimensionless group defined by Eq. (5)
σ	Dimensionless group defined by Eq. (4)

Theoretical

The results of the theoretical analysis (*5*) can be summarized by the following equations:

$$\text{Conversion} = 1 - \frac{p_o}{p_i} = 1 - \exp\left[-\frac{\kappa_1 k' V_{liq}}{F} E_{ov}\right] \quad (1)$$

$$\frac{1}{E_{ov}} = \frac{1}{E_1} + \frac{1}{\eta_f} \quad (2)$$

$$E_1 \delta_{liq} = \frac{\epsilon_{liq}[\tanh \mu(1-\theta)/\mu] + [\tanh \sigma\theta/\sigma]}{1 + (\mu/\sigma\epsilon_{liq}) \tanh \sigma\theta \cdot \tanh \mu(1-\theta)} \quad (3)$$

$$\sigma^2 = \frac{k' l^2}{D_{liq}} \quad (4)$$

$$\mu^2 = \sigma^2 \frac{\epsilon_{liq}\kappa_1 D_{liq}}{\epsilon_{liq}\kappa_1 D_{liq} + \epsilon_{gas} D_{gas}} \quad (5)$$

$$\delta_{liq} = \theta + (1-\theta)\epsilon_{liq} \quad (6)$$

$$\theta = f(\delta_{liq}) = \delta_{liq}[1 - \exp(-a\delta_{liq}^n) + \exp(-a)] \quad (7)$$

which correspond to the model of an ideal liquid-filled macropore shown in Fig. 1. In these equations, p_i and p_o are the inlet and outlet partial pressures of the reactant, respectively; E_{ov} is the overall effectiveness factor; $1/\eta_f$ is the gas film diffusion resistance (*11*); E_1 is the effectiveness factor for the supported liquid-phase catalyst pellets; θ is defined in Fig. 1; and δ_{liq} is the experimental liquid loading within the catalyst pellets.

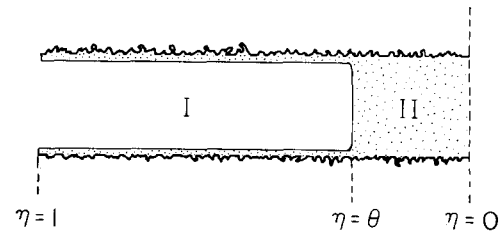

FIG. 1. Schematic diagram of an ideal liquid-filled macropore. The dimensionless parameter θ is the fraction of the total pore length that is occupied by a plug of liquid.

The remaining parameters in Eqs. (1) through (7) are defined in the Nomenclature section. The implications of these equations have already been summarized as follows (*5*):

"The behavior of a supported liquid-phase catalyst depends not only upon the amount of liquid dispersed within the porous solid, but also upon whether the dispersed liquid tends to form thin liquid films or liquid plugs. An extremely efficient SLPC results when only thin films or very small liquid 'micropools' are present throughout the porous structure. As the liquid loading increases, however, the pore passages become blocked with liquid and the SLPC activity reaches a maximum value. With a further increase in liquid loading the flooding of the pore passages becomes so severe that the SLPC activity progressively decreases,

a consequence of the long liquid diffusion paths. As can be observed in Eq. (1), the maximum is a consequence of the product of a linearly increasing function (V_{liq}) and a nonlinearly decreasing function (E_1)."

Experimental

Materials. The rhodium hydroformylation catalyst, $(Ph_3P)_2Rh(CO)Cl$, was prepared in this laboratory (*10*) according to the method of Chatt and Shaw (*12*). The $RhCl_3 \cdot 3H_2O$ and triphenylphosphine were purchased from the Mathey-Bishop Company and M & T Chemicals, Inc., respectively. Butyl benzyl phthalate (0.05 torr vapor pressure at 136°C) was obtained from Monsanto. Chloroform (Mallinckrodt analytical reagent) was used without further purification. The porous support was a 3/10 mesh Davison grade 70 granular silica gel which had the following measured physical properties: surface area, 340 m^2/g; particle density, 0.678 g/cm^3; true density, 2.19 g/cm^3; total pore volume, 1.018 cm^3/g; and macropore volume (diam. $\geq$ 700 Å), 0.038 cm^3/g.

Catalyst preparation. In the preparation of the catalyst solution, 74.2 mg of the rhodium catalyst and 1.57 g of triphenylphosphine were added to 23.1 g of butyl benzyl phthalate; the resulting mixture was heated for 3 hr over a steam bath to dissolve the solids. The density of the catalyst solution at 136°C was 1.056 g/cm^3. The catalyst solution was diluted with chloroform in the proportions shown in Table 1 and the resulting solution added to the amount of silica gel indicated. The solid–liquid composite was dried in a vacuum oven at room temperature to drive off the volatile solvent. Appropriate amounts of the dried catalyst (corresponding to 0.323 ± 0.016 cm^3 total pore volume on a dry basis) were charged into a 10-cm ½-inch od stainless steel reaction tube. A presaturator bed (benzyl butyl phthalate dispersed in silica gel) and an absorber bed (dry silica gel) were placed before and after the catalyst bed, respectively. From Table 2, it is clear that little interchange of solvent occurred among the three beds during the course of the reaction.

TABLE 1
Preparation of $Rh(Ph_3P)_2(CO)Cl$ Supported Liquid-Phase Catalysts with Different Liquid Loadings

Catalyst	δ_{liq} at 136°C[a]	Silica gel (g)	$CHCl_3$ (g)	Catalyst solution (g)
A	0.22	2.0032	2.9639	0.4698
B	0.33	2.0000	2.6252	0.6996
C	0.54	2.0084	1.7457	1.1617
D	0.70	2.0033	1.3953	1.5151
E	0.87	2.2111	0.3716	2.0690
F	0.97	2.0023	0.5405	2.0801

[a] Calculated from the equation, δ_{liq} = (g cat solution)/(1.018)(1.056)(g silica gel).

TABLE 2
Weights of Catalyst, Presaturator, and Absorber before and after Hydroformylation Studies

Catalyst	Catalyst		Presaturator		Absorber	
	Initial wt (mg)	Wt loss (mg)	Initial Wt (mg)	Wt loss (mg)	Initial wt (mg)	Wt gain (mg)
A	390.1	5.1	461.9	5.0	—	—
B	421.1	4.6	456.7	4.6	1432.1	64.5
C	498.0	2.7	454.9	7.4	—	—
D	556.3	2.9	460.9	5.9	1477.8	91.7
E	644.9	2.7	464.7	6.0	1464.0	50.6
F	614.1	3.1	445.3	5.8	1417.9	68.6

Apparatus and measurement procedure. The reaction tube was placed inside of a small thermostated reaction chamber equipped with a Nuclear Products Company fine metering valve (to control the gas flow) and a Carle Instruments, Inc. microvolume switching valve (to sample the effluent gas stream). The sampled gases were conveyed for analysis via a heated line to an Aerograph Model 600-D gas chromatograph equipped with an Infotronics digital readout system. The temperature inside the thermostated chamber was determined with a mercury thermometer; the temperature within the catalyst bed was not monitored. Sensitivity corrections for the raw chromatographic data were obtained from the tables of Dietz (*13*). Approximately 30 experimental measurements were made at each value of δ_{liq}—20 at the slow flow rate and 10 at the fast one. Each data point in Table 3 corresponds to an average of from three to

TABLE 3
SUMMARY OF CONVERSION, LOADING, AND FLOW DATA FOR HYDROFORMYLATION STUDIES

Catalyst	V_{pore} (cm³)	V_{liq} (cm³)	Slow flow rate F^a (cm³/sec)	Slow flow rate % Conversion n	Slow flow rate % Conversion iso	Fast flow rate F^a (cm³/sec)	Fast flow rate % Conversion n	Fast flow rate % Conversion iso
A	0.322	0.070	0.060	3.7	1.6	0.120	3.1	1.0
B	0.318	0.103	0.060	—	2.3	0.122	—	1.2
C	0.321	0.173	0.062	6.3	3.4	0.123	4.6	2.3
D	0.322	0.227	0.063	4.8	3.0	0.123	3.5	1.7
E	0.339	0.295	0.061	4.0	2.0	0.124	2.8	1.3
F	0.307	0.296	0.063	3.0	1.6	0.122	1.9	0.8

[a] At reactor conditions of 136°C and 490 psig. The gas composition was 6 mole% propylene, 47% hydrogen, and 47% carbon monoxide.

seven conversion measurements (the reproducibility of these measurements is indicated in Fig. 2). Periods of catalyst activation and deactivation were observed during each experimental run. The gas composition was 6 mole % propylene, 47% hydrogen, and 47% carbon monoxide.

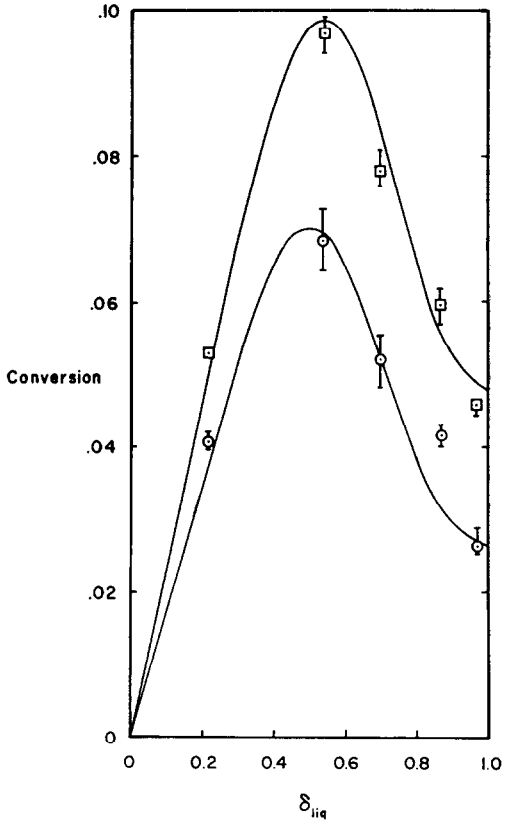

FIG. 2. Experimental points and theoretical conversion curves for the hydroformylation of propylene as a function of the liquid loading. The points ⊡ and ⊙, respectively, represent gas-phase flow rates of 0.062 and 0.122 cm³/sec.

RESULTS

Table 3 and Fig. 2 present experimental data for the loading, flow, and conversion of propylene to *n*-butyraldehyde and isobutyraldehyde. Although the reactor was run differentially, the Reynolds number was low and there was resistance to diffusion in the gas film external to the catalyst pellets. According to Eqs. (1) and (2), the conversion data therefore represent *lower limits* for the conversion of propylene to butyraldehyde at the reactor conditions indicated.

An attempt was made to correct the conversion data for the observed mass-transfer effects and to fit them to Eqs. (1) through (7). The quantity

$$\frac{1}{\kappa_1 k' E_{ov}} = -\frac{V_{liq}}{F \ln(p_o/p_i)} \tag{8}$$

was first calculated for all data points and plotted (Fig. 3). The gas film diffusion resistance for the slow flow rate was then calculated according to the equation

$$\left(\frac{1}{2\kappa_1 k' \eta_i}\right)_{\substack{\text{slow}\\\text{flow}\\\text{rate}}} = \left(\frac{1}{\kappa_1 k' E_{ov}}\right)_{\substack{\text{slow}\\\text{flow}\\\text{rate}}} - \left(\frac{1}{\kappa_1 k' E_{ov}}\right)_{\substack{\text{fast}\\\text{flow}\\\text{rate}}} \tag{9}$$

Repeated computer iterations based upon Eqs. (2), (3), and (7) finally yielded values for $\kappa_1 k'$, σ, and the curves for the effectiveness factor and the theoretical liquid loading as a

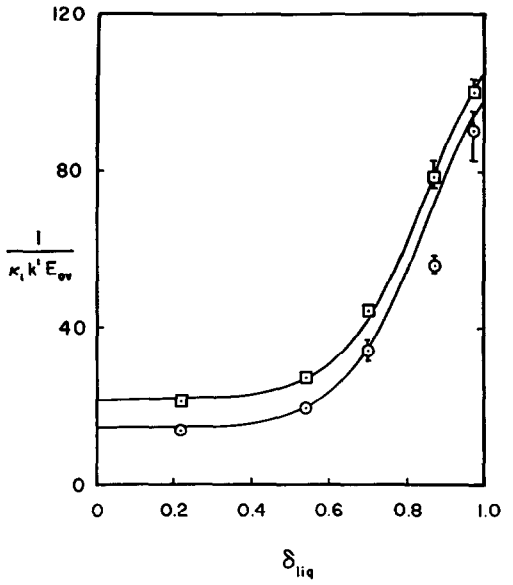

FIG. 3. Experimental points and theoretical curves for the quantity, $1/\kappa_1 k' E_{ov}$, as a function of liquid loading. The points ⊡ and ⊙, respectively, represent gas-phase flow rates of 0.062 and 0.122 cm³/sec.

function of the experimental liquid loading (Figs. 4 and 5). In Figs. 2 through 5, the points ⊙ and ⊡ are the experimental observations and the solid lines are the theoretical curves. It was no surprise that

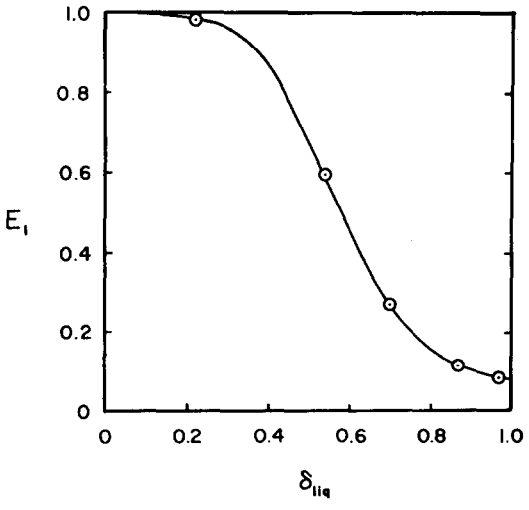

FIG. 4. Experimental points and theoretical curve for the effectiveness factor, E_1, as a function of liquid loading.

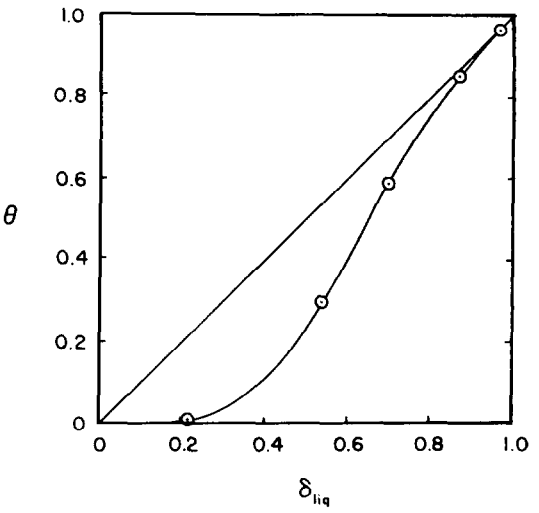

FIG. 5. Experimental points and theoretical curve for the theoretical liquid loading, θ, as a function of the experimental liquid loading, δ_{liq}. The curve corresponds to Eq. (7), where $a = 5.9$ and $n = 3.3$.

the experimental data could be fit so well, since a total of five empirical parameters were employed: $a = 5.9$ [Eq. (7)]; $n = 3.3$ [Eq. (7)]; $\eta_l = 0.5$ for the slow flow rate and 1.0 for the fast flow rate [Eq. (2)]; $\sigma = 12.4$ [Eq. (4)]; and $\kappa_1 k' = 0.137$ sec^{-1} cm^3 gas/cm^3 liq [Eq. (1)]. The initial concentration of the rhodium complex in these experiments was 4.6×10^{-3} M, so the specific activity was 30 M^{-1} sec^{-1}. Bis(triphenylphosphine) rhodium carbonyl chloride was therefore an exceptionally active hydroformylation catalyst.

DISCUSSION

The studies of the hydroformylation reaction described in this paper were of limited scope and designed simply to qualitatively verify the existence of a maximum in the conversion curve. A demonstration that Eqs. (1) through (7) are quantitatively verified by experiment must await more detailed experiments and independent determination of several physical parameters. For example, with longer catalyst beds and higher flow rates [or use of the wire-cage reactor of Simons and Tajbl (*14*)], the gas film diffusion resistance can be

eliminated from Eq. (1). Further, both $\kappa_1 k'$ and σ can be independently measured. The only empirical parameters are therefore a and n in Eq. (7).

It is quite likely that the same liquid-loading function, $f(\delta_{liq})$, will apply for a variety of liquid phases in a single type of porous support, so an independent confirmation of the functional form of Eq. (7) is also possible.

Supported liquid-phase catalysts are simple to prepare and are generally reproducible, provided that the soluble metal complex is stable under reaction conditions. We conclude that the preparation of a SLPC may eventually become a reliable method for measuring reaction rate constants in liquid phases at high temperatures and pressures, just as gas-liquid chromatography is presently being employed for the measurement of thermodynamic parameters (*15–17*) under similar conditions. In fact, the use of tracer gas-liquid chromatographic techniques (*18*) may complement the reactor studies of a SLPC by facilitating the measurement of the solubilities of the gaseous reactants in the supported liquid. The use of capillary columns (containing thin liquid films) may provide yet another alternative for the study of homogeneous liquid-phase reactions.

Acknowledgments

The author gratefully acknowledges many extensive discussions with J. F. Roth and the use of $(Ph_3P)_2Rh(CO)Cl$ prepared by F. Paulik.

References

1. Acres, G. J. K., Bond, G. C., Cooper, B. J., and Dawson, J. A., *J. Catalysis* **6**, 139 (1966).
2. Monsanto Co., Belgian Patent 711042 (1968); Bond, G. C., *Platinum Metals Rev.* **11**, 147 (1967).
3. Moravec, R. Z., Schelling, W. T., and Oldershaw, C. F., Brit. Patent 511,556 (1939); *Chem. Abstr.* **34**, 7102 (1940).
4. Moravec, R. Z., Schelling, W. T., and Oldershaw, C. F., Can. Patent 396,994 (1941); *Chem. Abstr.* **35**, 6103 (1941).
5. Rony, P. R., *Chem. Eng. Sci.* **23**, 1021 (1968).
6. Osborn, J. A., Wilkinson, G., and Young, J. F., *Chem. Commun.* p. 17 (1965).
7. Osborn, J. A., *Endeavor* **26**, 144 (1967).
8. Collman, J. P., *Accounts Chem. Res.* **1**, 136 (1968).
9. Osborn, J. A., Jardine, F. H., Young, J. F., and Wilkinson, G., *J. Chem. Soc.* (*A*), p. 1711 (1966).
10. Craddock, J. H., Hershman, A., Paulik, F. E., and Roth, J. F., *Ind. Eng. Chem.*, to be published.
11. Aris, R., *Chem. Eng. Sci.* **6**, 262 (1957).
12. Chatt, J., and Shaw, B. L., *J. Chem. Soc.* (*A*), p. 1437 (1966).
13. Dietz, W. A., *J. Gas Chromatog.* **5**, 68 (1967).
14. Carberry, J. J., *Ind. Eng. Chem.* **56**(11), 39 (1964).
15. Kobayashi, R., Chappelear, P. S., and Deans, H. A., *Ind. Eng. Chem.* **59**(10), 63 (1967).
16. Giddings, J. C., and Mallik, K. L., *Ind. Eng. Chem.* **59**(4), 18 (1967).
17. Young, C. L., *Chromatographic Rev.* **10**, 129 (1968).
18. Helfferich, F., and Peterson, D. L., *Science* **142**, 661 (1963).